DOI: 10.1002/ejic.200601028

Systematic Counterion Tuning of the Solid-State Structure of $[Pt(thiourea)_4]^{2+}$

Wolfgang Schiessl,[a] Ralph Puchta,[a,b] Živadin D. Bugarčić,[a,c] Frank W. Heinemann,[a] and Rudi van Eldik*[a]

Keywords: Counter ion / Conformers / Crystal engineering

Four different limiting molecular conformations are possible for the homoleptic square-planar complex tetrakis(thiourea)-platinum(II) depending on the up-down orientation of the four thiourea (TU) ligands with respect to the PtS_4 plane. The realization of all four possible conformers can be achieved by a systematic variation of the counter anion making use of their individual hydrogen bonding ability. In total, the molecular and crystal structures of seven tetrakis(thiourea)platinum(II) complexes were determined by X-ray diffraction. These are: $[Pt(TU)_4]Cl_2$, $[Pt(TU)_4]I_2$, $[Pt(TU)_4](CF_3SO_3)_2$, $[Pt(TU)_4](BPh_4)_2$, $[Pt(TU)_4](ClO_4)_2$, $[Pt(TU)_4]SiF_6{\cdot}0.25H_2O$ and $[Pt(TU)_4]S_2O_6$. In all cases thiourea is coordinated by the sulfur atom and the two amino groups are not involved in the complex formation. The four independent Pt–S distances do not differ significantly from each other with an average value of 2.324(3) Å. The coordination geometry around the platinum center is distorted square-planar. The orientation of the four TU groups in $[Pt(TU)_4]^{2+}$ depends on the molecular packing forces and hydrogen bonding ability of the counter anion. Hydrogen bonds of the type N–H···X (X = Cl^-, I^-, F^-, O and S) are observed.

Introduction

In contrast to its inertness as a metal, platinum and its compounds have become a major field of interest with respect to their possible applications. Besides the common usage of dispersed platinum metal as catalytic material in industrial processes,[1] Pt^{II} complexes are amongst the most commonly used antitumor drugs for certain types of cancer.[2] Intracellular thiols are known to play an important role in the metabolism of Pt antitumor drugs, since they are involved in trapping of the drug,[3] renal toxicity and other side-effects.[4] Thiourea (TU) is one of the best known nucleophiles for Pt^{II} complexes[5,6] and is commonly used in the investigation of ligand-substitution reactions in coordination chemistry. Moreover, thiourea can very easily displace other ligands from Pt^{II} complexes, including S-bonded ligands such as L-cysteine in $[Pt(terpy)(S\text{-}cys)]^+$ with a rate constant of 0.94 ± 0.02 $M^{-1}s^{-1}$ at 25 °C, and even much easier guanosine in $[Pt(terpy)(N7\text{-}guo)]^{2+}$ with a rate constant of 4.87 ± 0.03 $M^{-1}s^{-1}$.[7] The strong binding ability of S-donor nucleophiles can as well be used to reverse unwanted side-effects in chemotherapy.[8,9] It has been demonstrated that thiourea could restore the biological activity of platinated DNA.[10] Thiourea and other sulfur-containing compounds such as diethyl dithiocarbamate (DEDTC), sodium thiosulfate (STS), glutathione (GSH), *S*-2-(3-(aminopropylamino)ethylphosphorothioic acid (amifostine, WR-2721, Ethiol), methionine, cysteine, penicillamine, biotin, sodium 2-mercaptoethanesulfonate (mesna) and its oxidized S–S bridged dimer (di)mesna (BNP-7787), have been applied as rescue or protective agents, in order to reduce the toxicity of platinum antitumor complexes.[11,12,13] The protective effect of these compounds is either to prevent or to reverse the formation of Pt–S adducts in proteins.

Thiourea coordinates flexibly via the S-donor to the platinum center and the two amino groups are not involved in the complex formation.[14,15] For the proper interaction of drugs with purely organic material, the consideration of different conformations is very important, as the drugs have to fit inside the enzyme pocket.[16] Therefore, the question of conformers should also be addressed in the development of drug mimetics based on metal complexes. The NH_2 groups on thiourea can be utilized to form hydrogen-bonded mediated clusters together with suitable anions or other compounds, resulting in interesting structural host-guest motifs.[17] Furthermore, there is current interest in the design of selective receptors for anions,[18,19] which could interact through either electrostatic or hydrogen-bonding interactions.[20,21] The orientation of the four TU groups depends on the molecular packing forces and hydrogen bonding. In the following, these conformers are referred to as OOOO, IOOO, IIOO and IOIO with respect to the flip-flop orientation of the thiourea ligands as shown in Figure 1. Although most of these conformers have been re-

[a] Institute for Inorganic Chemistry, University of Erlangen-Nürnberg,
Egerlandstrasse 1, 91058 Erlangen, Germany
[b] Computer Chemistry Center, University of Erlangen-Nürnberg, Nägelsbachstr. 25, 91052 Erlangen, Germany
[c] Department of Chemistry, Faculty of Science, University of Kragujevac,
P. O. Box 60, 34000 Kragujevac, Serbia
Supporting information for this article is available on the WWW under http://www.eurjic.org or from the author.

ported individually as part of studies focusing on other topics,[22,23,24] we will show in the present study that all four possible conformers of the $[Pt(TU)_4]^{2+}$ unit can be realized by systematic tuning of the molecular structure by the hydrogen-bonding ability of the inorganic counter anion exclusively, without the need of organic substances or additional solvent species as frame works.

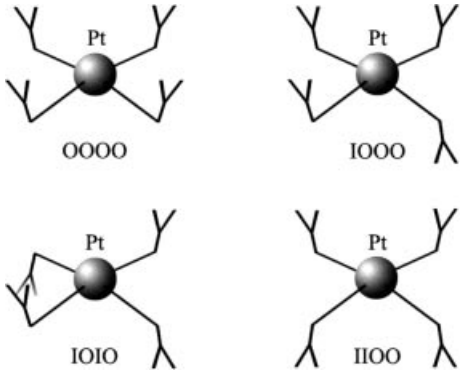

Figure 1. Schematic overview and definition of abbreviations for the four possible $[Pt(TU)_4]^{2+}$ conformers.

As part of our interest in the synthesis, structure and reactivity of coordination complexes of Pd^{II} and Pt^{II}, we report here a systematic and detailed study of the crystal structures of $[Pt(TU)_4]X_n$, where X represents the counterions Cl^-, I^-, $CF_3SO_3^-$, BPh_4^- and ClO_4^- (n = 2), and $S_2O_8^{2-}$ and SiF_6^{2-} (n = 1), in an attempt to gain information on the crystal packing, hydrogen bonding network and orientation of the four TU ligands as a function of the selected counterion.

Results and Discussion

Theoretical Calculations

Three of the four possible conformers were calculated applying symmetry constrains. The non-symmetrical IOOO (C_1), calculated without symmetry constrains, changed its conformation during the structure optimization and became the energetically most favorable IOIO. On the one hand we attribute this to the low energy barrier for rotation along the Pt–S bond, on the other hand it emphasizes the influence of the counterion. The moderate energy differences between the three conformers (IOIO 0 kcal/mol, IIOO 2 kcal/mol and OOOO 8 kcal/mol) in the gas phase[25] (see Figure 2 and Table 1) are in a range that can be exceeded by extra stabilization via hydrogen bonding. On the basis of 5 to 10 kcal/mol per hydrogen bond in the solid state,[26] already one or two hydrogen bonds should be able to overcome the calculated energy barrier between the different conformers. Since in every $[Pt(TU)_4]^{2+}$ motif 16 H_{N-H} are available for possible hydrogen bond formation, the TU moieties are forced into their respective orientation.

In order to support a distinctive hydrogen network, we selected in addition to halogen anions also oxo and per-

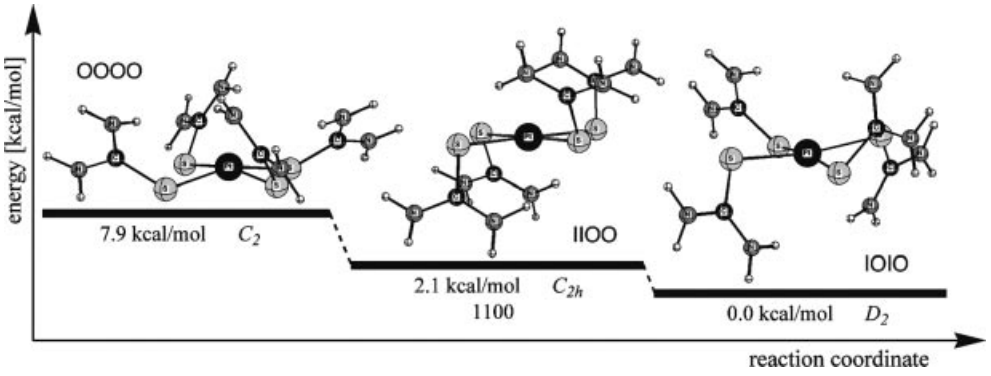

Figure 2. Optimized (RB3LYP/LANL2DZp) structures of the $[Pt(TU)_4]^{2+}$ conformers. (Pt: large black circles, C: small black circles, N: dark grey circles, S: light grey circles, H: white circles).

Table 1. Summary of the calculated (RB3LYP/LANL2DZp) structures of the $[Pt(TU)_4]^{2+}$ conformers.

	OOOO	IIOO	IOIO
Point group	C_2	C_{2h}	D_2
Relative energies (RB3LYP/LANL2DZp) [kcal/mol]	7.9	2.1	0.0
Relative energies (RB3LYP/LACV3P+**) [kcal/mol]	7.6	1.7	0.0
S–Pt (RB3LYP/LANL2DZp) [Å]	2.41, 2.42, 2.41, 2.42	2.43, 2.43, 2.43, 2.43	2.42, 2.42, 2.42, 2.42
Pt deviation of S_4 plane (RB3LYP/LANL2DZp) [Å]	0.30	0.00	0.00
C–S–Pt angle	111.3, 116.6, 111.3	110.9, 110.9, 110.9	111.0, 111.0, 111.0
(RB3LYP/LANL2DZp) [°]	116.6	110.9	111.0
S–Pt–S angle (RB3LYP/LANL2DZp) [°]	91.7, 86.6, 91.7, 86.6	83.9, 96.2, 83.9, 96.2	97.4, 82.8, 97.4, 82.8
X–S···S–C angle	149.1, 138.1, 149.1	–85.8, 127.0, 85.8	–128.7, 88.1, –128.7
(RB3LYP/LANL2DZp) [°][a]	138.1	–127.0	88.1

[a] X = center of least square plane through the four coordinating sulfur atoms.

fluoro anions, viz. ClO_4^-, $S_2O_6^{2-}$, SiF_6^{2-} and $CF_3SO_3^-$. Whereas the halogen anions have the rotational symmetric K_h point group, the oxo and perfluoro anions have different symmetry groups with corresponding subgroups. The basic idea was to utilize these symmetry elements to stabilize the suggested $[Pt(TU)_4]^{2+}$ rotamers. In order to obtain the conformational structure of $[Pt(TU)_4]^{2+}$ in the absence of a hydrogen bonding network with the anions, we used $[B(Ph)_4]^-$ as a counterion. As summarized in Table 1, the Pt–S bonds in all conformers are almost identical with 2.42 Å, the Pt^{II} is ideally square-planar coordinated by the four S-donors (except in OOOO) and the C=S–Pt^{II} shows equivalent angles of 111°. The distortion in the OOOO conformer can be explained in terms of only two TU ligands that have a NH-group showing a common orientation toward a neighboring thiourea sulfur (NH···S 2.48 Å), whereas the other two TU exhibit a contact toward their own S atom.

Crystallographic Results

The molecular structures of the $[Pt(TU)_4]^{2+}$ cations in the complexes $[Pt(TU)_4]SiF_6{\cdot}0.25H_2O$, $[Pt(TU)_4]S_2O_6$, $[Pt(TU)_4](ClO_4)_2$, $[Pt(TU)_4]I_2$, $[Pt(TU)_4](BPh_4)_2$, $[Pt(TU)_4](CF_3SO_3)_2$ and $[Pt(TU)_4]Cl_2$ are shown in Figures 3, 4, 5, and 6 (see also Figures S1 to S3 in the Supporting Information). Selected bond lengths and angles for the various $[Pt(TU)]X_n$ complexes are given in Tables 2, 3, 4, 5, 6, 7, and 8.

In general, TU is coordinated to Pt via its sulfur donor in all the $[Pt(TU)_4]^{2+}$ cations. The coordination geometry around the platinum center is distorted square-planar.

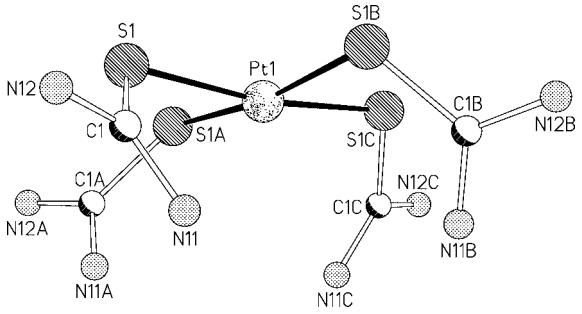

Figure 3. Molecular structure of the $[Pt(TU)_4]^{2+}$ cation of the complex $[Pt(TU)_4]SiF_6{\cdot}0.25H_2O$, (OOOO).

Table 2. Selected bond lengths [Å] and angles [°] for $[Pt(TU)_4]Cl_2$ (IOIO).

Pt(1)–S(1)	2.3168(7)	Pt(1)–S(2)	2.3222(6)
Pt(1)–S(3)	2.3308(7)	Pt(1)–S(4)	2.3344(6)
S(1)–C(1)	1.732(3)	C(1)–N(12)	1.310(3)
C(1)–N(11)	1.324(3)	S(2)–C(2)	1.730(3)
C(2)–N(21)	1.316(3)	C(2)–N(22)	1.336(3)
S(3)–C(3)	1.740(2)	C(3)–N(31)	1.313(3)
C(3)–N(32)	1.321(3)	S(4)–C(4)	1.739(3)
C(4)–N(42)	1.316(3)	C(4)–N(41)	1.317(3)
S(1)–Pt(1)–S(2)	83.75(2)	S(1)–Pt(1)–S(3)	174.46(2)
S(2)–Pt(1)–S(3)	91.84(2)	S(1)–Pt(1)–S(4)	98.84(2)
S(2)–Pt(1)–S(4)	175.79(2)	S(3)–Pt(1)–S(4)	85.76(2)
C(1)–S(1)–Pt(1)	110.77(9)	N(12)–C(1)–N(11)	120.7(2)
N(12)–C(1)–S(1)	123.0(2)	N(11)–C(1)–S(1)	116.4(2)
C(2)–S(2)–Pt(1)	109.42(9)	N(21)–C(2)–N(22)	119.4(2)
N(21)–C(2)–S(2)	124.3(2)	N(22)–C(2)–S(2)	118.3(2)

Hydrogen bonds for $[Pt(TU)_4]Cl_2$

D–H···A	*d*(D–H)	*d*(H···A)	*d*(D···A)	<(DHA)
N(11)–H(11B)···Cl(2)#1	0.88	2.48	3.329(2)	161.9
N(11)–H(11A)···S(3)#2	0.88	2.59	3.434(2)	159.9
N(12)–H(12B)···Cl(1)	0.88	2.67	3.347(2)	134.9
N(12)–H(12B)···S(4)	0.88	2.74	3.396(2)	132.6
N(12)–H(12A)···Cl(1)#3	0.88	2.44	3.236(2)	151.0
N(21)–H(21B)···S(3)	0.88	2.72	3.352(2)	130.2
N(21)–H(21B)···Cl(2)	0.88	2.74	3.505(2)	146.8
N(21)–H(21A)···Cl(2)#4	0.88	2.46	3.508(2)	161.7
N(22)–H(22B)···Cl(1)#5	0.88	2.58	3.384(2)	151.8
N(22)–H(22A)···S(4)#6	0.88	2.88	3.681(2)	152.5
N(31)–H(31A)···Cl(2)#7	0.88	2.48	3.262(2)	147.8
N(31)–H(31B)···Cl(1)	0.88	2.63	3.293(2)	133.5
N(32)–H(32B)···Cl(1)#8	0.88	2.41	3.254(2)	162.1
N(32)–H(32A)···Cl(2)#7	0.88	2.49	3.263(2)	147.5
N(41)–H(41B)···S(1)	0.88	2.42	3.240(2)	154.7
N(41)–H(41A)···Cl(1)#9	0.88	2.59	3.385(2)	150.3
N(41)–H(41A)···S(2)#1	0.88	2.97	3.515(2)	121.9
N(42)–H(42A)···Cl(1)#9	0.88	2.44	3.272(2)	157.1
N(42)–H(42B)···Cl(2)#10	0.88	2.28	3.144(2)	166.2

Symmetry transformations used to generate equivalent atoms: #1 $-x+1, -y+1, -z$; #2 $x, -y+1/2, z-1/2$; #3 $-x, -y, -z$; #4 $-x+1, y+1/2, -z+1/2$; #5 $-x, -y+1, -z$; #6 $x, y+1, z$; #7 $x-1, y, z$; #8 $-x, y+1/2, -z+1/2$; #9 $x+1, y, z$; #10 $-x+1, y-1/2, -z+1/2$

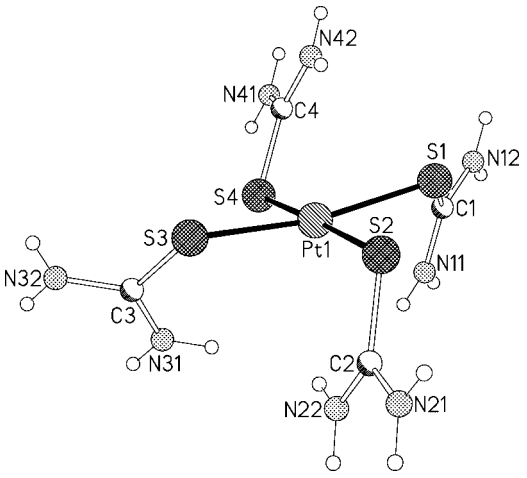

Figure 4. Molecular structure of the $[Pt(TU)_4]^{2+}$ cation of the complex $[Pt(TU)_4]S_2O_6$, (IOOO).

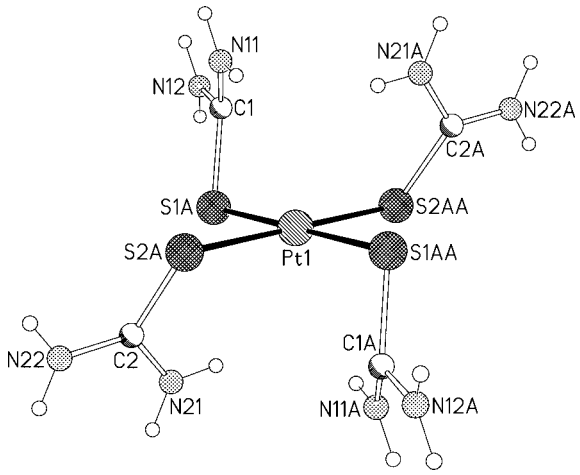

Figure 5. Molecular structure of the $[Pt(TU)_4]^{2+}$ cation of the complex $[Pt(TU)_4](ClO_4)_2$, (IIOO).

Whereas in most of the complexes the largest deviation from the optimum value of 90° for the S–Pt–S angle is less than 4.5°, significantly larger angles of 101.68(2)° in $[Pt(TU)_4](CF_3SO_3)_2$ and 98.84(2)° in $[Pt(TU)_4]Cl_2$ indicate a stronger distortion of the square planar arrangement, which is in good agreement with literature values reported for the chloride complex, viz. 98.3(02)°[14] and 98.9(1)°.[15] The central Pt atom in all investigated complexes is situated well within the S_4 plane; the only significant displacement of the Pt center from the square plane is observed for the complex in $[Pt(TU)_4]SiF_6$ [0.180(1) Å] and $[Pt(TU)_4]S_2O_6$ [0.091(1) Å].

The thiourea ligands are arranged in a rotor-like fashion with respect to the PtS_4 plane, independent of whether they point upwards or downwards. The dihedral angle between the PtS_4 plane and a least-squares plane calculated through the thiourea ligand unit $S=C(N_2)$ varies between 35.3(1)° and 85.2(2)°, with an overall average of 64.9°. The four Pt–S distances in each of the $[Pt(TU)_4]^{2+}$ units do not differ much from each other (see Tables 2, 3, 4, 5, 6, 7, and 8) and cover the narrow range from 2.313(2) Å (shortest distance found in $[Pt(TU)_4](ClO_4)_2$) to 2.345(1) Å (longest distance found in $[Pt(TU)_4](BPh_4)_2$). The overall average value calculated for all Pt–S bond lengths for all investigated $[Pt(TU)_4]X_n$ complexes amounts to 2.324(3) Å. This is in very good

Table 3. Selected bond lengths [Å] and angles [°] for $[Pt(TU)_4]SiF_6 \cdot 0.25H_2O$ (OOOO).

Pt(1)–S(1)#1	2.3149(7)	Pt(1)–S(1)#2	2.3149(7)
Pt(1)–S(1)#3	2.3149(7)	Pt(1)–S(1)	2.3149(7)
S(1)–C(1)	1.735(3)	C(1)–N(11)	1.319(3)
C(1)–N(12)	1.321(3)	Si(1)–F(13)#2	1.683(2)
Si(1)–F(13)#3	1.683(2)	Si(1)–F(13)#1	1.683(2)
Si(1)–F(13)	1.683(2)	Si(1)–F(11)	1.685(3)
Si(1)–F(12)	1.703(3)	N(11)–H(11A)	0.8800
S(1)#1–Pt(1)–S(1)#2	89.654(3)	S(1)#1–Pt(1)–S(1)#3	89.654(3)
S(1)#2–Pt(1)–S(1)#3	171.09(3)	S(1)#1–Pt(1)–S(1)	171.09(3)
S(1)#2–Pt(1)–S(1)	89.654(3)	S(1)#3–Pt(1)–S(1)	89.654(3)
C(1)–S(1)–Pt(1)	110.67(9)	N(11)–C(1)–N(12)	120.0(2)
N(11)–C(1)–S(1)	122.9(2)	N(12)–C(1)–S(1)	117.1(2)
C(1)–N(11)–H(11A)	120.0	C(1)–N(11)–H(11B)	120.0
F(13)#2–Si(1)–F(13)#3	179.61(2)	F(13)#2–Si(1)–F(13)#1	89.999(1)
F(13)#3–Si(1)–F(13)	89.999(1)	F(13)#1–Si(1)–F(13)	179.6(2)

Symmetry transformations used to generate equivalent atoms: #1 $-x+1/2, -y+1/2, z$; #2 $-y+1/2, x, z$; #3 $y, -x+1/2, z$

Hydrogen bonds for $[Pt(TU)_4]SiF_6 \cdot 0.25H_2O$ (OOOO)

D–H···A	*d*(D–H)	*d*(H···A)	*d*(D···A)	<(DHA)
N(11)–H(11A)···F(13)#4	0.88	2.07	2.882(3)	153.7
N(11)–H(11B)···F(12)	0.88	2.11	2.942(3)	157.9
N(12)–H(12A)···F(11)#5	0.88	2.25	2.975(3)	139.2
N(12)–H(12A)···F(13)#6	0.88	2.32	3.142(3)	154.7
N(12)–H(12B)···S(1)#7	0.88	2.71	3.451(3)	143.2
N(12)–H(21B)···S(1)#8	0.88	2.97	3.563(3)	126.6
O(1)–H(1A)···F(13)#8	0.85	2.27	3.118(2)	180.0

Symmetry transformations used to generate equivalent atoms: #1 $-x+1/2, -y+1/2, -z$; #2 $-y+1/2, x, z$; #3 $y, -x+1/2, z$; #4 $x+1/2, -y+1, -z+1/$; #5 $-x+1, y+1/2, -x+1/2$; #6 $-y+1, -x+1, -x+1/2$; #7 $-y+1, x+1/2, -z$; #8 $-x+1/2, -y+3/2, z$

Table 4. Selected bond lengths [Å] and angles [°] for $[Pt(TU)_4]S_2O_6$ (IOOO).

Pt(1)–S(4)	2.313(2)	Pt(1)–S(3)	2.321(1)
Pt(1)–S(1)	2.321(2)	Pt(1)–S(2)	2.344(2)
S(1)–C(1)	1.740(4)	C(1)–N(11)	1.319(5)
C(1)–N(12)	1.320(5)	S(2)–C(2)	1.730(5)
C(2)–N(21)	1.315(5)	C(2)–N(22)	1.325(6)
S(3)–C(3)	1.738(5)	C(3)–N(31)	1.316(6)
C(3)–N(32)	1.319(6)	S(4)–C(4)	1.732(4)
C(4)–N(41)	1.312(5)	C(4)–N(42)	1.319(5)
S(4)–Pt(1)–S(3)	90.58(4)	S(4)–Pt(1)–S(1)	93.69(4)
S(3)–Pt(1)–S(1)	168.03(4)	S(4)–Pt(1)–S(2)	177.71(4)
S(3)–Pt(1)–S(2)	89.67(4)	S(1)–Pt(1)–S(2)	86.51(4)
C(1)–S(1)–Pt(1)	111.0(2)	N(11)–C(1)–N(12)	120.0(4)
N(11)–C(1)–S(1)	122.5(3)	N(12)–C(1)–S(1)	117.2(3)
C(2)–S(2)–Pt(1)	107.8(2)	N(21)–C(2)–N(22)	118.5(4)
N(21)–C(2)–S(2)	118.6(4)	N(22)–C(2)–S(2)	122.8(3)

Hydrogen bonds for $[Pt(TU)_4]S_2O_6$ D–H···A	*d*(D–H)	*d*(H···A)	*d*(D···A)	<(DHA)
N(11)–H(11A)···O(63)#1	0.88	2.12	2.988(4)	169.9
N(11)–H(11B)···O(53)#2	0.88	2.23	3.069(4)	159.4
N(12)–H(12A)···O(61)#1	0.88	2.20	3.075(5)	178.2
N(12)–H(12B)···O(51)#3	0.88	2.47	3.173(5)	137.0
N(21)–H(21A)···O(52)#4	0.88	2.21	2.971(5)	143.9
N(21)–H(21B)···O(61)#5	0.88	2.04	2.907(5)	167.3
N(22)–H(22B)···O(53)#2	0.88	2.26	3.030(5)	146.3
N(22)–H(22A)···S(3)#4	0.88	2.96	3.565(4)	127.4
N(31)–H(31A)···O(62)#6	0.88	2.10	2.957(5)	163.3
N(31)–H(31B)···O(53)#2	0.88	2.13	2.979(5)	161.4
N(31)–H(31B)···S(5)#2	0.88	2.94	3.608(4)	134.6
N(32)–H(32)···O(63)#6	0.88	2.13	3.005(5)	169.9
N(32)–H(32)···O(52)	0.88	2.20	2.924(5)	139.4
N(41)–H(41A)···O(62)#7	0.88	2.29	2.996(5)	137.8
N(41)–H(41B)···S(1)#8	0.88	2.57	3.408(4)	160.0
N(41)–H(41B)···S(2)#8	0.88	2.93	3.524(4)	126.4
N(42)–H(42A)···O(51)#3	0.88	2.40	2.931(5)	119.0
N(42)–H(42B)···S(1)	0.88	2.84	3.268(4)	111.3
N(42)–H(42B)···S(3)#9	0.88	2.70	3.366(4)	133.6

Symmetry transformations used to generate equivalent atoms: #1 $-x+1, -y+1/2, -z+3/2$; #2 $-x+1/2, -y+1, z+1/2$; #3 $-x+3/2, -y+1, z+1/2$; #4 $x-1/2, -y+3/2, -z+1$; #5 $x, y+1, z$; #6 $x-1/2, -y+1/2, -z+1$; #7 $x+1/2, -y+1/2, -z+1$; #8 $-x+1, y-1/2, -z+3/2$; #9 $x+1/2, -y+3/2, -z+1$

agreement with earlier published results (2.324 Å) for $[Pt(TU)]Cl_2$,[15] and is only slightly longer than earlier published data (2.313 Å) for the same complex.[14]

Whereas the parameters for the central PtS_4 unit are basically the same for all investigated $[Pt(TU)_4]^{2+}$ cations, remarkable differences are observed for the orientation of the four thiourea ligands with respect to the PtS_4 plane that results in one of the conformations OOOO, IOOO, IIOO or IOIO.

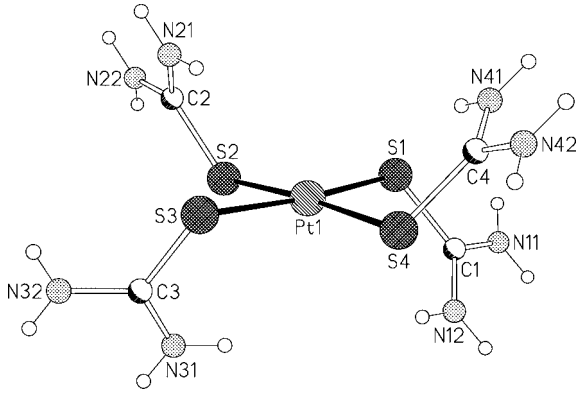

Figure 6. Molecular structure of the $[Pt(TU)_4]^{2+}$ cation of the complex $[Pt(TU)_4]Cl_2$, (IOIO).

$[Pt(TU)_4]SiF_6 \cdot 0.25H_2O$, Conformation OOOO

Both the $[Pt(TU)_4]^{2+}$ cation and the SiF_6^{2-} anion are situated on a crystallographic fourfold rotation axis (C_4 molecule symmetry).[27] Within the crystal the anion is situated exactly above and below the PtS_4 plane of the cation (Figure 7), with distances between the axial fluorine atoms (F12 and F11A) and Pt of 3.125(2) and 4.562(2) Å, respectively. The short Pt···F12 distance reflects the fact that F12 is involved in strong hydrogen bonding (Table 3) acting as a fourfold acceptor, thus forcing the OOOO conformation of the cation with the NH_2 groups of the thiourea ligands as hydrogen-bond donors. The hydrogen-bond acceptor function of F12 results in a significant longer Si–F bond (1.703(2) Å vs. an average of 1.683(3) Å for the other five Si–F distances). In contrast to these strong intermolecular

Table 5. Selected bond lengths [Å] and angles [°] for $[Pt(TU)_4](ClO_4)_2$ (IIOO).

Pt(1)–S(1B)#1	2.313(2)	Pt(1)–S(1B)	2.313(2)
Pt(1)–S(2A)#1	2.313(2)	Pt(1)–S(2A)	2.313(2)
Pt(1)–S(2B)	2.330(2)	Pt(1)–S(2B)#1	2.330(2)
Pt(1)–S(1A)#1	2.338(2)	Pt(1)–S(1A)	2.338(2)
S(1)–C(1)	1.819(5)	S(1B)–C(1)	1.734(5)
C(1)–N(11)	1.253(6)	C(1)–N(12)	1.330(6)
S(2A)–C(2)	1.802(5)	S(2B)–C(2)	1.782(5)
C(2)–N(21)	1.274(6)	C(2)–N(22)	1.309(6)
Pt(2)–S(4B)#2	2.308(3)	Pt(2)–S(4B)	2.308(3)
Pt(2)–S(4A)	2.320(3)	Pt(2)–S(4A)#2	2.320(3)
Pt(2)–S(3B)	2.328(3)	Pt(2)–S(3B)#2	2.328(3)
Pt(2)–S(3A)	2.331(3)	Pt(2)–S(3A)#2	2.331(3)
S(3A)–C(3)	1.689(5)	S(3B)–C(3)	1.806(6)
C(3)–N(31)	1.325(6)	C(3)–N(32)	1.326(7)
S(4A)–C(4)	1.800(6)	S(4B)–C(4)	1.715(5)
S(1B)#1–Pt(1)–S(1B)	180.0	S(1B)#1–Pt(1)–S(2A)#1	124.61(8)
S(1B)–Pt(1)–S(2A)#1	55.39(8)	S(1B)#1–Pt(1)–S(2A)	55.39(8)
S(1B)–Pt(1)–S(2A)	124.61(8)	S(2A)#1–Pt(1)–S(2A)	180.0
S(1B)#1–Pt(1)–S(2B)	87.91(8)	S(1B)–Pt(1)–S(2B)	92.09(8)
S(2A)#1–Pt(1)–S(2B)	147.33(8)	S(2A)–Pt(1)–S(2B)	32.67(8)
S(1B)#1–Pt(1)–S(2B)#1	92.09(8)	S(1B)–Pt(1)–S(2B)#1	87.91(8)
S(2A)#1–Pt(1)–S(2B)#1	32.67(8)	S(2A)–Pt(1)–S(2B)#1	147.33(8)
S(2B)–Pt(1)–S(2B)#1	180.0	S(1B)#1–Pt(1)–S(1A)#1	34.08(8)
S(1B)#1–Pt(1)–S(1A)#1	145.92(8)	S(2A)#1–Pt(1)–S(1A)#1	91.89(8)
S(2A)–Pt(1)–S(1A)#1	88.11(8)	S(2B)–Pt(1)–S(1A)#1	120.69(8)
S(2B)#1–Pt(1)–S(1A)#1	59.31(8)	S(1B)#1–Pt(1)–S(1A)	145.92(8)
S(1B)–Pt(1)–S(1A)	34.08(8)	S(2A)#1–Pt(1)–S(1A)	88.11(8)
S(2A)–Pt(1)–S(1A)	91.89(8)	S(2B)–Pt(1)–S(1A)	59.31(8)
S(2B)#1–Pt(1)–S(1A)	120.69(8)	S(1A)#1–Pt(1)–S(1A)	180.0

Symmetry transformations used to generate equivalent atoms: #1 $-x+1, -y+1, -z+1$; #2 $-x, -y+1, -z$

Hydrogen bonds for $[Pt(TU)_4](ClO_4)_2$

D–H···A	*d*(D–H)	*d*(H···A)	*d*(D···A)	<(DHA)
N(11)–H(11A)···O(12)#3	0.88	2.36	3.137(5)	147.2
N(11)–H(11A)···O(21)#4	0.88	2.50	3.126(5)	128.6
N(12)–H(12B)···O(13)	0.88	2.34	3.156(5)	155.1
N(12)–H(12A)···O(14)#3	0.88	2.23	3.055(5)	156.8
N(12)–H(12B)···S(4B)#5	0.88	2.62	3.485(9)	169.1
N(21)–H(21A)···O(22)#6	0.88	2.55	2.997(5)	112.3
N(21)–H(21A)···O(23)#2	0.88	2.55	3.217(5)	133.0
N(21)–H(21A)···O(21)#2	0.88	2.56	3.083(5)	119.1
N(21)–H(21B)···O(13)#1	0.88	2.20	3.004(5)	151.9
N(21)–H(21B)···S(1A)	0.88	3.01	3.477(4)	115.5
N(22)–H(22A)···O(11)#7	0.88	2.47	3.176(2)	137.3
N(22)–H(22A)···O(23)#2	0.88	2.51	3.179(5)	133.4
N(22)–H(22B)···S(2A)#7	0.88	2.40	3.264(5)	166.4
N(31)–H(31A)···O(23)#8	0.88	2.55	3.254(6)	137.7
N(31)–H(31B)···S(2B)	0.88	2.49	3.175(6)	135.6
N(31)–H(31B)···S(2A)	0.88	2.96	3.805(6)	161.2
N(32)–H(32A)···O(23)#8	0.88	2.32	3.080(5)	144.1
N(32)–H(32A)···O(11)#3	0.88	2.53	3.104(5)	123.6
N(32)–H(32B)···O(24)	0.88	2.22	3.032(6)	154.2
N(41)–H(41A)···O(12)#9	0.88	2.14	3.014(4)	176.5
N(41)–H(41B)···O(24)	0.88	2.37	3.187(5)	154.7
N(41)–H(41B)···S(3B)#2	0.88	2.93	3.433(5)	118.3
N(42)–H(42A)···O(21)#10	0.88	2.22	3.005(5)	148.1
N(42)–H(42B)···S(4B)#5	0.88	2.64	3.511(5)	169.5
N(42)–H(42B)···S(4A)#5	0.88	2.80	3.644(6)	160.5

Symmetry transformations used to generate equivalent atoms: #1 $-x+1, -y+1, -z+1$; #2 $-x, -y+1, -z$; #3 $x, -y+3/2, -z-1/2$; #4 $x+1, -y+3/2, z+1/2$; #5 $-x+1, -y+1, -z$; #6 $-x, y-1/2, -z+1/2$; #7 $-x, -y+1, -z+1$; #8 $x, -y+3/2, z+1/2$; #9 $-x, y, z-1$; #10 $x+1, y, z$

hydrogen bridges, intramolecular N–H···S hydrogen bonding seems to play only a minor role (H···S distances of 3.12 Å and N–H···S angles of 102.8°).

Within the crystal packing each SiF_6^{2-} anion connects four neighbored $[Pt(TU)_4]^{2+}$ cations via intermolecular N–H···S hydrogen bonds with the equatorial F13 atoms always

Table 6. Selected bond lengths [Å] and angles [°] for $[Pt(TU)_4]I_2$ (IOIO).

Pt(1)–S(2)	2.327(2)	Pt(1)–S(2)#1	2.327(2)
Pt(1)–S(1)	2.334(2)	Pt(1)–S(2)#1	2.334(2)
S(1)–C(1)	1.724(6)	C(1)–N(12)	1.322(8)
C(1)–N(11)	1.327(8)	S(2)–C(2)	1.720(6)
C(2)–N(22)	1.321(8)	C(2)–N(21)	1.330(8)
Pt(2)–S(3)#2	2.326(2)	Pt(2)–S(3)	2.326(2)
Pt(2)–S(4)#2	2.329(2)	Pt(2)–S(4)	2.329(2)
S(3)–C(3)	1.717(6)	C(3)–N(31)	1.320(8)
C(3)–N(32)	1.326(8)	S(4)–C(4)	1.725(6)
C(4)–N(41)	1.323(8)	C(4)–N(42)	1.315(8)
S(2)–Pt(1)–S(2)#1	180.000(1)	S(2)–Pt(1)–S(1)	87.75(6)
S(2)#1–Pt(1)–S(1)	92.25(6)	S(2)–Pt(1)–S(1)#1	92.25(6)
S(2)#1–Pt(1)–S(1)#1	87.75(6)	S(1)–Pt(1)–S(1)#1	180.0
S(3)#2–Pt(2)–S(3)	180.1(2)	S(3)#2–Pt(2)–S(4)#2	87.37(6)
S(3)–Pt(2)–S(4)#2	92.63(6)	S(3)#2–Pt(2)–S(4)	92.63(6)
S(3)–Pt(2)–S(4)	87.37(6)	S(4)#2–Pt(2)–S(4)	180.00(7)
C(3)–S(3)–Pt(2)	107.5(2)	N(31)–C(3)–N(32)	119.2(5)
C(1)–S(1)–Pt(1)	107.0(2)	N(12)–C(1)–N(11)	119.3(6)
N(12)–C(1)–S(1)	123.0(5)	N(11)–C(1)–S(1)	117.7(5)
C(2)–S(2)–Pt(1)	109.2(2)	N(22)–C(2)–N(21)	119.2(6)
N(22)–C(2)–S(2)	122.8(5)	N(21)–C(2)–S(2)	118.0(5)

Symmetry transformations used to generate equivalent atoms: #1 $-x+1, -y+1, -z+1$; #2 $-x, -y, -z$

Hydrogen bonds for $[Pt(TU)_4]I_2$

D–H···A	*d*(D–H)	*d*(H···A)	*d*(D···A)	<(DHA)
N(11)–H(11A)···I(2)#3	0.88	2.76	3.603(5)	159.6
N(11)–H(11B)···I(2)#4	0.88	2.83	3.616(5)	149.3
N(12)–H(12A)···I(1)#3	0.88	3.08	3.657(5)	125.0
N(12)–H(12A)···I(2)#3	0.88	3.17	3.925(5)	145.1
N(12)–H(12B)···I(1)	0.88	2.88	3.654(5)	147.8
N(21)–H(21A)···S(3)#5	0.88	2.98	3.742(6)	145.5
N(21)–H(21B)···I(1)#5	0.88	2.79	3.670(6)	173.5
N(22)–H(22A)···S(3)#5	0.88	2.57	3.419(5)	163.1
N(22)–H(22B)···I(1)	0.88	2.79	3.564(5)	147.5
N(22)–H(22B)···S(1)#1	0.88	2.88	3.288(5)	110.3
N(31)–H(31A)···I(2)#6	0.88	2.94	3.654(5)	139.2
N(31)–H(31B)···I(2)#7	0.88	2.87	3.657(5)	152.3
N(32)–H(32A)···I(1)#6	0.88	2.68	3.535(6)	164.3
N(32)–H(32B)···I(1)#8	0.88	2.76	3.604(6)	160.6
N(41)–H(41B)···I(2)#2	0.88	2.78	3.639(5)	166.3
N(42)–H(42A)···S(1)#9	0.88	2.62	3.462(5)	160.6
N(42)–H(42B)···I(2)#7	0.88	2.75	3.547(5)	151.4
N(42)–H(42B)···S(3)#2	0.88	2.97	3.392(5)	111.4

Symmetry transformations used to generate equivalent atoms: #1 $-x+1, -y+1, -z+1$; #2 $-x, -y, -z$; #3 $-x+1, -y, -z+1$; #4 $x, y, z+$; #5 $x+1, y, z$; #6 $x, y-1, z$; #7 $-x+1, -y, -z$; #9 $-x, -y, -z+1$; #9 $x, y-1, z-1$

being the acceptor. Thus, two-dimensional double layers of cations and anions are formed with an up-side (O) face-to-face arrangement of the cations and the anions being located in between. These double layers are linked further by additional intermolecular N–H···S bridges to complete the three-dimensional hydrogen bond network (Figure 8). From the refinement results we concluded the presence of not more than 1/4 water molecule per complex unit. This only partially occupied water molecule is located at a position that allows for the formation of hydrogen bonds to four neighboring SiF_6^{2-} anions depending on the orientation of the H_2O (being situated in the special position *4a* of the space group leading to rotational disorder). This enables the water molecule to further interconnect the anions within layers parallel to the crystallographic *ab* plane (see Figure 8).

$[Pt(TU)_4]S_2O_6$, Conformation IOOO

The $[Pt(TU)_4]^{2+}$ cation has C_1 symmetry and the $S_2O_6^{2-}$ anion is situated above the PtS_4 plane with three of the thiourea groups pointing upwards (Figure 9). The dithionate anion is connected to the cation by three hydrogen bonds with the O53 atom acting as acceptor resulting in a Pt–O53 distance of 3.394(3) Å. The fourth down-oriented thiourea ligand is involved in a moderate to strong intramolecular hydrogen bond (N42–H42B···S1) with a donor acceptor distance N42···S1 of 3.268(4) Å (Table 5). Other possible intramolecular hydrogen bonds may be present but are significantly weaker having either longer N···S distances (3.691(4), 4.999(4) Å] or much less favorable N–H···S angles (98.9(1)°]. Each of the eight NH_2 groups of the $[Pt(TU)_4]^{2+}$ cation is involved in two or three hydrogen bridges

Table 7. Selected bond length [Å] and angles [°] for $[Pt(TU)_4](CF_3SO_3)_2$ (IIOO).

Pt(1)–S(2)	2.3153(7)	Pt(1)–S(3)	2.3161(7)
Pt(1)–S(1)	2.3175(7)	Pt(1)–S(4)	2.3229(7)
S(1)–C(1)	1.730(3)	C(1)–N(12)	1.317(3)
C(1)–N(11)	1.317(3)	S(2)–C(2)	1.726(3)
C(2)–N(22)	1.317(3)	C(2)–N(21)	1.322(3)
S(3)–C(3)	1.734(3)	C(3)–N(31)	1.307(4)
C(3)–N(32)	1.313(4)	S(4)–C(4)	1.720(3)
C(4)–N(42)	1.314(3)	C(4)–N(41)	1.331(3)
S(5)–O(53)	1.438(2)	S(5)–O(51)	1.443(2)
S(5)–O(52)	1.448(2)	S(5)–C(5)	1.820(3)
C(5)–F(51)	1.323(4)	C(5)–F(53)	1.330(4)
C(5)–F(52)	1.332(3)	S(6)–O(61)	1.439(2)
S(6)–O(63)	1.442(2)	S(6)–O(62)	1.4460(2)
S(6)–C(6)	1.821(3)	C(6)–F(62)	1.327(3)
C(6)–F(63)	1.329(3)	C(6)–F(61)	1.330(3)
S(2)–Pt(1)–S(3)	101.68(2)	S(2)–Pt(1)–S(1)	86.03(2)
S(3)–Pt(1)–S(1)	172.26(2)	S(2)–Pt(1)–S(4)	174.32(2)
S(3)–Pt(1)–S(4)	83.97(2)	S(1)–Pt(1)–S(4)	88.31(2)
C(1)–S(1)–Pt(1)	107.20(9)	N(12)–C(1)–N(11)	119.5(2)
N(12)–C(1)–S(1)	118.0(2)	N(11)–C(1)–S(1)	122.5(2)
C(2)–S(2)–Pt(1)	109.59(9)	N(22)–C(2)–N(21)	119.6(2)
N(22)–C(2)–S(2)	123.8(2)	N(21)–C(2)–S(2)	116.6(2)
C(3)–S(3)–Pt(1)	117.50(9)	N(31)–C(3)–N(32)	119.8(3)
N(31)–C(3)–S(3)	124.1(2)	N(32)–C(3)–S(3)	116.0(2)
C(4)–S(4)–Pt(1)	106.79	N(42)–C(4)–N(41)	119.0(2)
N(42)–C(4)–S(4)	123.5(2)	N(41)–C(4)–S(4)	117.5(2)

Hydrogen bonds for $[Pt(TU)_4](CF_3SO_3)_2$

D–H···A	*d*(D–H)	*d*(H···A)	*d*(D···A)	<(DHA)
N(11)–H(11A)···O(63)#1	0.88	2.14	2.981(3)	159.6
N(11)–H(11B)···O(61)	0.88	2.23	2.855(3)	128.1
N(12)–H(12A)···O(61)#1	0.88	2.19	3.006(3)	154.4
N(12)–H(12A)···S(6)#1	0.88	2.95	3.788(2)	159.6
N(12)–H(12B)···O(63)	0.88	2.08	2.850(3)	145.1
N(21)–H(21A)···O(62)#3	0.88	2.28	3.016(3)	141.5
N(21)–H(21A)···S(3)#3	0.88	2.84	3.533(2)	137.0
N(21)–H(21B)···O(51)#4	0.88	2.20	3.032(3)	156.5
N(22)–H(22A)···S(4)#3	0.88	2.82	3.626(2)	152.5
N(22)–H(22B)···O(62)	0.88	2.49	3.169(3)	134.9
N(22)–H(22B)···S(3)	0.88	2.72	3.428(2)	138.7
N(31)–H(31A)···O(53)#5	0.88	2.14	3.020(3)	176.2
N(31)–H(31B)···O(53)	0.88	2.51	3.119(3)	126.9
N(31)–H(31B)···S(2)	0.88	2.69	3.324(2)	129.5
N(32)–H(32A)···O(52)#5	0.88	2.13	2.979(3)	161.0
N(32)–H(32A)···S(5)#5	0.88	2.94	3.784(3)	162.6
N(32)–H(32B)···F(53)#6	0.88	2.52	3.065(4)	120.9
N(41)–H(41A)···O(51)#7	0.88	2.22	3.017(3)	149.9
N(41)–H(41A)···S(5)#7	0.88	2.91	3.753(2)	161.4
N(41)–H(41B)···O(62)#8	0.88	2.08	2.927(3)	160.0
N(42)–H(42A)···O(52)#7	0.88	2.24	3.085(3)	160.3
N(42)–H(42B)···O(51)	0.88	2.56	3.241(3)	134.4

Symmetry transformations used to generate equivalent atoms: #1 $-x+1, y-1/2, -z+3/2$; #2 $x, y-1, z$; #3 $x, -y+5/2, z+1/2$; #4 $x, -y+3/2, z+1/2$; #5 $-x, -y+2, -z+1$; #6 $x, y+1, z$; #7 $x, -y+3/2, z-1/2$; #8 $x, -y+5/2, z-1/2$

(Table 4). The remaining five O atoms of the $S_2O_6^{2-}$ anion act as acceptors for two hydrogen bonds each. Interestingly, one $S_2O_6^{2-}$ anion forms hydrogen bonds to six different cations, thus controlling the packing arrangement.

Within the crystal packing the $[Pt(TU)_4]^{2+}$ cations form zig-zag chains along the crystallographic *b* direction, the cations being connected by intermolecular N–H···S hydrogen bridges with S1, S2 and S3 acting as acceptors, while S4 is only involved in the above mentioned intramolecular H bond. The zig-zag chains form a herringbone arrangement with the $S_2O_6^{2-}$ anions occupying the resulting channels (Figure 10).

$[Pt(TU)_4](ClO_4)_2$, Conformation IIOO

The $[Pt(TU)_4]^{2+}$ cation is situated on a crystallographic inversion center and, consequently, has C_i symmetry. Similar to the observation made for the OOOO-type complex $[Pt(TU)_4]SiF_6$, the ClO_4^- anions are again arranged above

Table 8. Selected bond lengths [Å] and angles [°] for $[Pt(TU)_4](BPh_4)_2$ (IOIO).

Pt(1)–S(1)#1	2.3226(8)	Pt(1)–S(1)	2.3226(8)
Pt(1)–S(2)#1	2.3451(8)	Pt(1)–S(2)	2.3451(8)
S(1)–C(1)	1.719(3)	C(1)–N(11)	1.322(4)
C(1)–N(12)	1.322(4)	N(11)–H(11A)	0.8800
N(11)–H(11B)	0.8800	N(12)–H(12A)	0.8800
N(12)–H(12B)	0.8800	S(2)–C(2)	1.718(3)
C(2)–N(22)	1.314(4)	C(2)–N(21)	1.327(4)
N(21)–H(21A)	0.8800	N(21)–H(21B)	0.8800
N(22)–H(22A)	0.8800	N(22)–H(22B)	0.8800
B(1)–C(41)	1.637(4)	B(1)–C(21)	1.642(4)
B(1)–C(11)	1.843(4)	B(1)–C(31)	1.650(4)
C(11)–C(16)	1.401(4)	C(11)–C(12)	1.411(4)
C(12)–C(13)	1.380	C(12)–H(12A)	0.9500
C(13)–C(14)	1.398(4)	C(13)–H(13A)	0.9500
C(14)–C(15)	1.384(4)	C(14)–H(14A)	0.9500
C(15)–C(16)	1.400(4)	C(15)–H(15A)	0.9500
S(1)#1–Pt(1)–S(1)	180.00(4)	S(1)#1–Pt(1)–S(2)#1	94.46(3)
S(1)–Pt(1)–S(2)#1	85.54(3)	S(1)#1–Pt(1)–S(2)	85.54(3)
S(1)–Pt(1)–S(2)	94.46(3)	S(2)#1–Pt(1)–S(2)	180.0
C(1)–S(1)–Pt(1)	111.9(2)	N(11)–C(1)–N(12)	118.8(3)
N(11)–C(1)–S(1)	117.8(2)	N(12)–C(1)–S(1)	123.3(2)
C(1)–N(11)–N(11A)	120.0	C(1)–N(11)–H(11B)	120.0
H(11A)–N(11)–H(11B)	120.0	C(1)–N(12)–H(12A)	120.0
C(1)–N(12)–H(12B)	120.0	H(12A)–N(12)–H(12B)	120.0
C(2)–S(2)–Pt(1)	110.3(2)	N(22)–C(2)–N(21)	120.1(3)
N(22)–C(2)–S(2)	122.4(3)	N(21)–C(2)–S(2)	117.5(3)
C(2)–N(21)–H(21A)	120.0	C(2)–N(21)–H(21B)	120.0
H(21A)–N(21)–H(21B)	120.0	C(2)–N(22)–H(21A)	120.0
C(2)–N(22)–H(22B)	120.0	H(22A)–N(22)–H(22B)	120.0
C(41)–B(1)–C(21)	113.6(2)	C(41)–B(1)–C(11)	105.6(2)
C(21)–B(1)–C(11)	111.8(2)	C(41)–B(1)–C(31)	108.5(2)
C(21)–B(1)–C(31)	105.9(2)	C(11)–B(1)–C(31)	111.5(2)
C(16)–C(11)–C(12)	115.0(3)	C(16)–C(11)–B(1)	124.9(3)
C(12)–C(11)–B(1)	120.1(3)	C(13)–C(12)–C(11)	123.1(3)
C(12)–C(13)–C(14)	120.2(3)	C(12)–C(13)–H(13A)	119.9
C(14)–C(13)–H(13A)	119.9	C(15)–C(14)–C(13)	118.8(3)
C(15)–C(14)–H(14A)	120.6	C(13)–C(14)–H(14A)	120.6

Symmetry transformations used to generate equivalent atoms: #1 $-x, -y+1, -z+1$

Hydrogen bond for $[Pt(TU)_4](BPh_4)_2$

D–H···A	*d*(D–H)	*d*(H···A)	*d*(D···A)	<(DHA)
N(12)–H(12B)···S(2)	0.88	2.75	3.182(3)	112.0
N(22)–H(22B)···S(1A)#1	0.88	3.33	3.745(3)	111.4

Symmetry transformations used to generate equivalent atoms: #1 $-x, -y+1, -z+1$

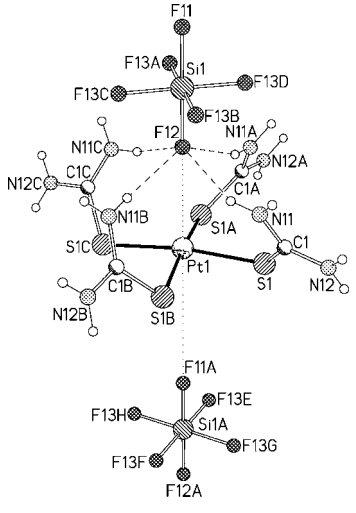

Figure 7. Conformation and H-bonding in $[Pt(TU)_4]SiF_6 \cdot 0.25H_2O$ (OOOO).

and below the PtS_4 plane of the $[Pt(TU)_4]^{2+}$ cation, but now form a significantly tilted angle. The angle between the perpendicular axis to the PtS_4 plane and the O···Pt···O line amounts to 22.4(1)°, and the corresponding O13···Pt1–S angles are 74.6(1)° (S1A), 73.6(1)° (S2A), 105.4(1)° (S1AA) and 106.4(1)° (S2AA). The oxygen atoms O13 and O13A both act as acceptors for two hydrogen bridges to the up- and down-oriented thiourea ligands (Figure 11), and the distance between Pt and the two symmetry related oxygen atoms O13 and O13A is 3.352(3) Å. Though the asymmetric part of the unit cell contains two independent molecules that are both subjected to disorder with two alternative positions for each of the sulfur atoms, the same arrangement of cations and anions is observed for both. Only one significant intramolecular hydrogen bond is observed in each of the two independent cations, viz. N21–H21B···S1A and N41A–H41B···S3A (see Table 5).

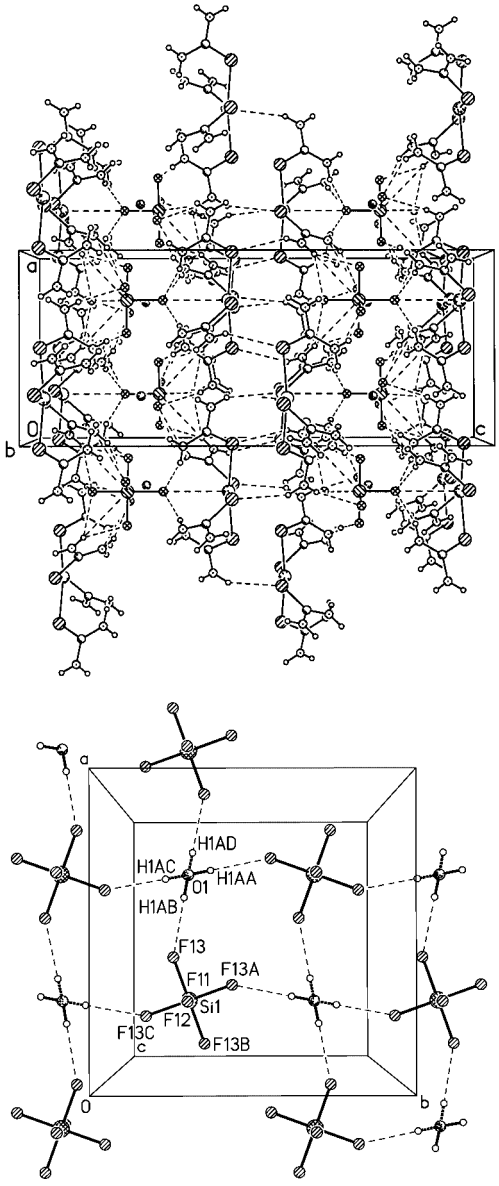

Figure 8. Crystal packing of $[Pt(TU)_4]SiF_6 \cdot 0.25H_2O$ (top) and crystal packing details of $[Pt(TU)_4]SiF_6 \cdot 0.25H_2O$ (bottom) highlighting the intermolecular hydrogen bonds between the partially occupied and disordered water molecules and the SiF_6^{2-} anions parallel to the crystallographic *ab* plane (dashed solid lines between O and H atoms indicate the alternative orientation for the water molecule resulting from symmetry requirements).

The crystal packing is characterized by layers of $[Pt(TU)_4]^{2+}$ cations perpendicular to the *c* direction. Within these layers the cations are connected via intermolecular N–H···S hydrogen bridges. The space between the cation layers is occupied by the ClO_4^- anions connecting the layers via intermolecular N–H···O hydrogen bridges (see Figure 12 and Table 5).

$[Pt(TU)_4]Cl_2$, Conformation IOIO

We have re-examined the previously reported X-ray structure of $[Pt(TU)_4]Cl_2$.[14,15,22] The $[Pt(TU)_4]^{2+}$ cation in

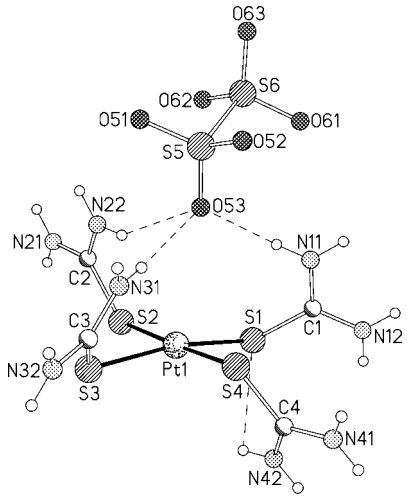

Figure 9. Conformation and H-bonding in $[Pt(TU)_4]S_2O_6$ (IOOO).

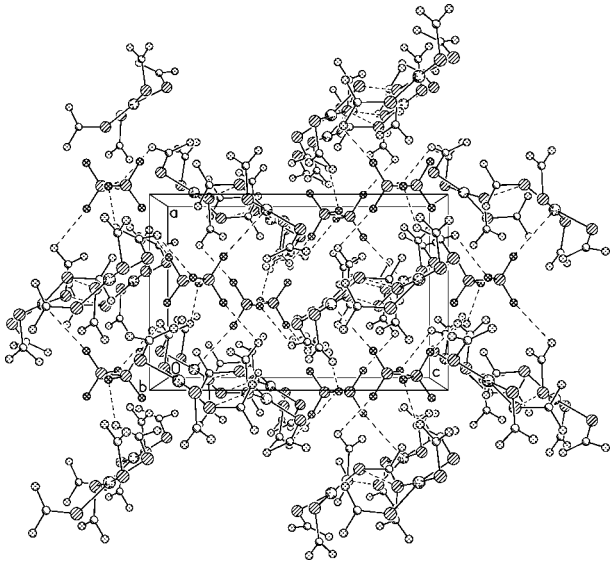

Figure 10. Crystal packing of $[Pt(TU)_4]S_2O_6$.

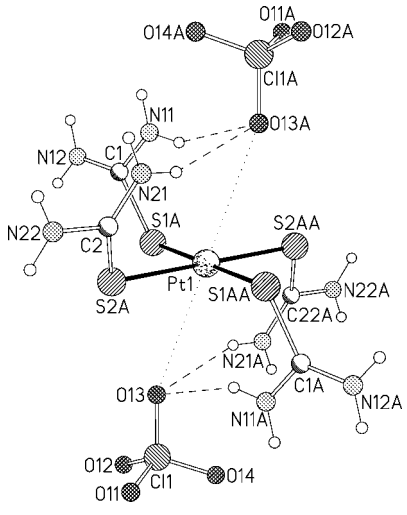

Figure 11. Conformation and H-bonding in $[Pt(TU)_4](ClO_4)_2$.

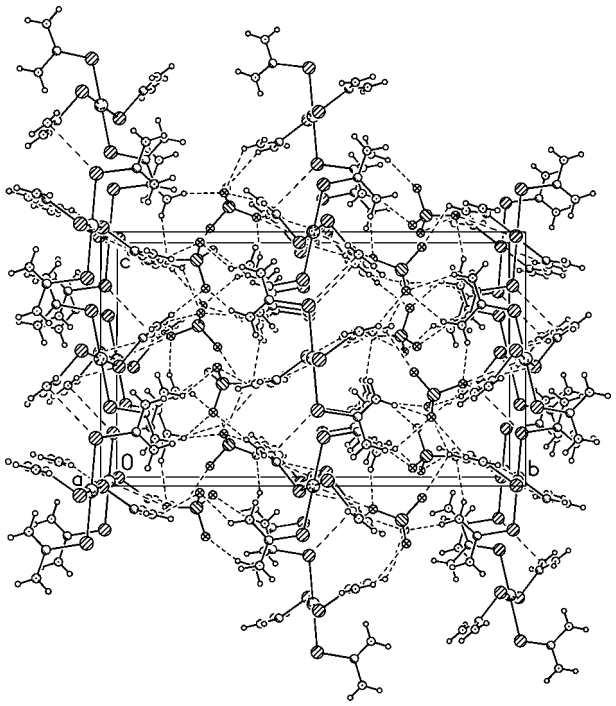

Figure 12. Crystal packing of $[Pt(TU)_4](ClO_4)_2$.

this molecular structure has only C_1 symmetry and shows significant deviation from the ideal square planar arrangement as is indicated by the S–Pt–S angles [largest deviation from 90° is observed for S1–Pt1–S4: 98.84(2)°]. The Cl^- anions are situated above and below the PtS_4 plane but do not form a straight line with the Pt center any longer, the Cl1···Pt1···Cl2 angle being now 130.16(1)° instead of 180° in the SiF_6^- and ClO_4^- salts. Significant differences are observed for the two Pt···Cl distances [Pt1···Cl1 4.143(1) Å vs. Pt1···Cl2 3.727(1) Å]. Whereas Girling et al.[14] report five and three hydrogen bonds for the two halogen anions, respectively, our data indicate only two hydrogen bonds formed to the above the PtS_4 plane positioned chloride anion Cl1 and only one to the below the plane situated single Cl2. Consistent with other findings in the literature,[15] intramolecular N–H···S hydrogen bonding seems to have a stronger effect on the conformation here (see Figure 13 and Table 2). Besides comparably short H···S and N···S distances, the N–H···S angles (> 130°) become more favorable for effective hydrogen bonding.

Within the crystal the $[Pt(TU)_4]^{2+}$ cations are linked by intermolecular N–H···S hydrogen bridges and form stacks running along the crystallographic *a* axis. Each of the Cl^- ions is linked to five neighbored cations by intermolecular N–H···Cl bridges and connects the cation stacks to complete the three-dimensional hydrogen bonding network of the crystal structure (see Figure 14 and Table 2).

$[Pt(TU)_4](BPh_4)_2$, Conformation IIOO

The molecular and crystal structure of this compound is interesting since the BPh_4^- anion cannot act as a hydrogen-

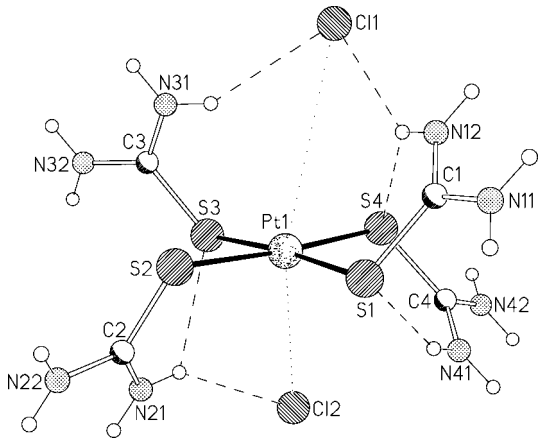

Figure 13. Conformation and H-bonding in $[Pt(TU)_4]Cl_2$.

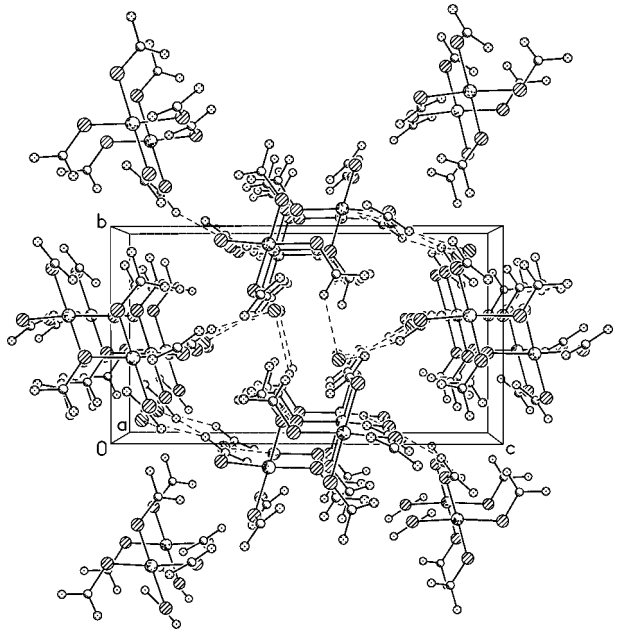

Figure 14. Crystal packing of $[Pt(TU)_4]Cl_2$.

bond acceptor. The $[Pt(TU)_4]^{2+}$ cation has crystallographically imposed C_i symmetry. The rotor-like arrangement of the thiourea ligands with respect to the PtS_4 plane features two smaller and two larger dihedral angles of 49.1(1)° and 79.2(1)°, respectively. Surprisingly, intramolecular hydrogen bonds seem to play only a minor role. According to the parameters, only two of them can be mentioned here (Table 8). The crystalline packing can be described as hexagonal close packing of the BPh_4^- anions, whereas the $[Pt(TU)_4]^{2+}$ cations occupy one half of the octahedral interstices.

$[Pt(TU)_4]I_2$ and $[Pt(TU)_4](CF_3SO_3)_2$, Conformation IIOO

In these two crystal structures the structural motif of the arrangement of the two anions above and below the $[Pt(TU)_4]^{2+}$ moiety is repeated (see $[Pt(TU)_4](ClO_4)_2$). In the iodide compound the corresponding tilt angle between

the perpendicular axis to the PtS_4 plane and the I···Pt···I line amounts to 22.5(1)°, whereas this angle is 18.4(1)° in the triflate compound (using the sulfur atoms of the two anions for the construction of the line). In both compounds again numerous intermolecular N–H···S bridges force the formation of cation layers. The anions are situated in the space between the layers and connect these by intermolecular hydrogen bonds of the N–H···I or N–H···O and N–H···F type, respectively (see Tables 6 and 7).

Conclusions

Seven $[Pt(TU)_4]X_n$ (X = Cl^-, I^-, $CF_3SO_3^-$, BPh_4^- and ClO_4^- (n = 2), and $S_2O_8^{2-}$ and SiF_6^{2-} (n = 1)) complexes were synthesized and their crystal structures were determined by X-ray diffraction. Theoretical calculations show that the possible limiting conformations for the $[Pt(TU)_4]^{2+}$ moiety have only moderate energy differences (OOOO: 7.9 kcal/mol, IIOO: 2.1 kcal/mol (relative energy differences compared to the IOIO conformer)). These energy differences can be overcome by efficient hydrogen bonding, in which each of the NH_2 groups of the thiourea ligand can act as hydrogen-bond donor, provided the counterions can serve as acceptors. Consequently, the realization of the four theoretically limiting conformations (OOOO, IOOO, IIOO, IOIO) was achieved by the use of different counterions. Whereas the highly symmetrical SiF_6^{2-} di-anion forced the formation of the all-up conformation (OOOO) using its ability to act as acceptor for four individual equidistant N–H···F hydrogen bridges, the use of other anions resulted in less symmetrical molecular structures. The use of $S_2O_6^{2-}$, the second di-anion in the group of anions in this study leads to the formation of the IOOO conformer of the $[Pt(TU)_4]^{2+}$ cation with three practically equivalent N–H···O hydrogen bridges to one oxygen atom (O53) of the dithionate acting as acceptor, and the remaining five oxygens being involved in an extensive hydrogen bonding network connecting cations and anions. ClO_4^-, $CF_3SO_3^-$ and I^- as mono-anions all created an analogous structural motif with one anion above and one below the PtS_4 plane, but with a significant tilt angle of roughly 20° between the X···Pt···X line and the perpendicular axis to the PtS_4 plane. The resulting arrangement of cation-anion hydrogen interactions leads to the formation of the IIOO conformer in these three crystal structures. The IIOO conformer was also realized in the complex $[Pt(TU)_4](BPh_4)_2$, but without having the possibility of forming intermolecular cation-anion hydrogen bridges. Though intramolecular hydrogen bond formation would be an alternative in the BPh_4^- salt, and is indeed observed to a more or less extent in all investigated $[Pt(TU)_4]^{2+}$ cations, no significantly stronger intramolecular hydrogen bonds have been observed here. From the parameters, a more pronounced influence of intramolecular hydrogen bonding can be attributed to the complex $[Pt(TU)_4]Cl_2$ having the smallest anion and exhibiting the IOIO conformation of the $[Pt(TU)_4]^{2+}$ cation.

Due to the small energy differences between the four limiting conformers, the choice of a suitable anion in terms of size, hydrogen-bond acceptor ability and/or symmetry can force the formation of either of the OOOO, IOOO, IIOO, or IOIO conformers in the solid state.

Quantum Chemical Methods

We performed RB3LYP[28,29,30]/LANL2DZp[31,32,33,34] hybrid density functional calculations, i.e., with pseudo-potentials on the heavy elements and the valence basis set augmented with polarization functions.[35,36] In addition, we used RB3LYP/LACV3P+**,[32,33,34,37] a basis set originally developed by Schrödinger Inc. Structures were characterized as minima by computation of vibrational frequencies. Relative energies were corrected for zero point vibrational energy. The GAUSSIAN 03 suite of programs was used.[38]

Experimental Section

Thiourea (Merck, p.a. quality grade) and $K_2[PtCl_4]$ (Johnson Matthey) were of the highest purity commercially available and used as received.

Tetrakis(thiourea)platinum(II) Chloride, $[Pt(TU)_4]Cl_2$: Preparation according to a previously published method.[39] $C_4H_{16}Cl_2N_8PtS_4$ (570.46): Calcd. C 8.42, H 2.83, N 19.64, S 22.48; found: C 8.43, H 2.74, N 19.45, S 22.32.

Tetrakis(thiourea)platinum(II) Dithionate, $[Pt(TU)_4]S_2O_6$: An acidic aqueous solution (pH 2) of $K_2[PtCl_4]$ (0.2 mM) and thiourea (10 mM) was heated under reflux for 12 h. After formation of the tetrakis(thiourea)platinum(II) complex, the solution was concentrated by a factor of 10 and an equal aliquot of a saturated solution of $Na_2S_2O_6$ was added. Single crystals of $[Pt(TU)_4]S_2O_6$ were obtained by slow evaporation of the solution. Elemental analysis could not be performed due to a very low yield of crystals.

Tetrakis(thiourea)platinum(II) Hexafluorosilicate, $[Pt(TU)_4]SiF_6 \cdot 0.25H_2O$: Crystal preparation was done as described above with a saturated solution of Na_2SiF_6, and single crystals were obtained within minutes after the saturated counterion solution was added. $C_{16}H_{66}F_{24}N_{32}OPt_4S_{16}Si_4$ (2584.54): Calcd. C 7.44, H 2.57, N 17.34, S 19.85; found: C 7.52, H 2.59, N 17.02, S 20.00.

Crystal preparations for all the other complexes, **$[Pt(TU)_4](ClO_4)_2$**, **$[Pt(TU)_4]I_2$**, **$[Pt(TU)_4](CF_3SO_3)_2$**, and **$[Pt(TU)_4](BPh_4)_2$** were done as described above. The crystals suitable for X-ray measurements were obtained by crystallization from water and after cooling in a refrigerator.

$[Pt(TU)_4](ClO_4)_2$: $C_4H_{16}Cl_2N_8O_8PtS_4$ (698.46): Calcd. C 6.88, H 2.31, N 16.04, S 18.36; found: C 7.05, H 2.46, N 15.83, S 18.56.

$[Pt(TU)_4]I_2$: No elemental analysis due to a very low yield of crystals.

$[Pt(TU)_4](CF_3SO_3)_2$: $C_6H_{16}F_6N_8O_6PtS_6$ (797.68): Calcd. C 9.03, H 2.02, N 14.05, S 24.07; found: C 9.08, H 1.94, N 13.92, S 23.92.

$[Pt(TU)_4](BPh_4)_2$: $C_{52}H_{56}B_2N_8PtS_4$ (1138.02): Calcd. C 54.88, H 4.96, N 9.85, S 11.27; found: C 54.84, H 5.20, N 10.27, S 11.57.

X-ray Crystal Structure Determination of $[Pt(TU)_4]Cl_2$, $[Pt(TU)_4]I_2$, $[Pt(TU)_4](CF_3SO_3)_2$, $[Pt(TU)_4](BPh_4)_2$, $[Pt(TU)_4](ClO_4)_2$, $[Pt(TU)_4]$-

SiF_6·0.25H_2O and [Pt(TU)$_4$]S_2O_6: X-ray intensities were collected at 100 K on a Bruker-Nonius KappaCCD diffractometer using Mo-K_α radiation (λ = 0.71073 Å, graphite monochromator). Lorentz and polarization corrections were applied, absorption effects were corrected on the basis of multiple scans using SADABS[40] with the exception of [Pt(TU)$_4$](BPh_4)$_2$ where a numerical absorption correction was applied instead. All structures were solved by direct methods and refined using full-matrix least-squares procedures on F^2. All non-hydrogen atoms were refined with anisotropic displacement parameters. All hydrogen atoms are placed in positions calculated for optimized geometry, their isotropic displacement parameters were tied to those of their corresponding N

Table 9. Crystallographic data, data collection and crystal structure refinement details.

	[Pt(TU)$_4$]Cl_2	[Pt(TU)$_4$](ClO_4)$_2$	[Pt(TU)$_4$]S_2O_6	[Pt(TU)$_4$]SiF_6·0.25H_2O
Molecular formula	$C_4H_{16}Cl_2N_8PtS_4$	$C_4H_{16}Cl_2N_8O_8PtS_4$	$C_4H_{16}N_8O_6PtS_6$	$C_4H_{16.50}F_6N_8O_{0.25}PtS_4Si$
Formula weight	570.48	698.48	659.70	646.17
Temperature [K]	100(2)	100(2)	100(2)	100(2)
Crystal size (mm)	0.15 × 0.07 × 0.05	0.14 × 0.13 × 0.08	0.25 × 0.23 × 0.06	0.18 × 0.14 × 0.06
Crystal system	monoclinic	monoclinic	orthorhombic	tetragonal
Space group	$P2_1/c$	$P2_1/c$	$P2_12_12_1$[#]	$P4/ncc$
a [Å]	8.9859(4)	8.3650(5)	10.022(1)	9.1575(8)
b [Å]	10.1182(8)	19.696(2)	12.355(2)	9.1575(8)
c [Å]	18.206(2)	11.7678(7)	15.298(2)	22.155(2)
α [°]	90	90	90	90
β [°]	91.206(5)	90.819(5)	90	90
γ [°]	90	90	90	90
Volume [Å^3]	1654.9(2)	1938.6(3)	1894.2(4)	1857.9(3)
Z	4	4	4	4
Absorption coeff. μ [mm^{-1}]	9.305	7.997	8.109	8.131
$D_{calcd.}$ [Mg/m^3]	2.290	2.393	2.313	2.310
F(000)	1088	1344	1272	1234
θ range [°]	3.74 to 28.70	3.20 to 29.00	3.56 to 27.88	3.64 to 28.69
Reflections collected/unique	34570/4201 (R_{int} = 0.0422)	56744/5153 (R_{int} = 0.0651)	25408/4488 (R_{int} = 0.0588)	27855/1208 (R_{int} = 0.0444)
Reflections observed [$I > 2\sigma(I)$]	3614	3023	3913	1012
Goodness-of-fit on F^2	0.926	0.978	0.910	1.091
Final R indices [$I > 2\sigma(I)$]	R_1 = 0.0181 wR_2 = 0.0344	R_1 = 0.0256 wR_2 = 0.0425	R_1 = 0.0227 wR_2 = 0.0455	R_1 = 0.0178 wR_2 = 0.0347
R indices (all data)	R_1 = 0.0277 wR_2 = 0.0364	R_1 = 0.0723 wR_2 = 0.0513	R_1 = 0.0323 wR_2 = 0.0485	R_1 = 0.0273 wR_2 = 0.0368
Max. and min. transmission	0.628 and 0.421	0.527 and 0.325	0.615 and 0.156	0.614 and 0.301
[#] absolute structure (Flack) parameter: 0.025(5)				

	[Pt(TU)$_4$]I_2	[Pt(TU)$_4$](CF_3SO_3)$_2$	[Pt(TU)$_4$](BPh_4)$_2$
Molecular formula	$C_4H_{16}I_2N_8PtS_4$	$C_6H_{16}F_6N_8O_6PtS_6$	$C_{52}H_{56}B_2N_8PtS_4$
Formula weight	753.38	797.72	1138.00
Temperature [K]	100(2)	100(2)	100(2)
Crystal size (mm)	0.07 × 0.05 × 0.05	0.20 × 0.15 × 0.07	0.39 × 0.14 × 0.04
Crystal system	triclinic	monoclinic	monoclinic
Space group	$P\bar{1}$	$P2_1/c$	$P2_1/c$
a [Å]	9.0532(5)	19.336(2)	12.371(2)
b [Å]	9.2044(7)	10.248(1)	11.841(1)
c [Å]	13.0466(4)	12.422(2)	17.307(2)
α [°]	71.304(4)	90	90
β [°]	71.953(4)	104.80(1)	109.14(1)
γ [°]	63.351(5)	90	90
Volume [Å^3]	902.53(10)	2379.8(5)	2395.1(5)
Z	2	4	2
Absorption coeff. μ [mm^{-1}]	11.656	6.510	3.151
$D_{calcd.}$ [Mg/m^3]	2.772	2.226	1.578
F(000)	688	1536	1152
θ range [°]	3.33 to 27.10	3.82 to 27.10	3.06 to 27.10
Reflections collected/unique	20801/3976 (R_{int} = 0.0426)	56133/5228 (R_{int} = 0.0461)	53932/5269 (R_{int} = 0.0861)
Reflections observed [$I > 2\sigma(I)$]	3365	4561	4179
Goodness-of-fit on F^2	1.163	0.987	1.073
Final R indices [$I > 2\sigma(I)$]	R_1 = 0.0262 wR_2 = 0.0517	R_1 = 0.0185 wR_2 = 0.0351	R_1 = 0.0261 wR_2 = 0.0574
R indices (all data)	R_1 = 0.0375 wR_2 = 0.0540	R_1 = 0.0272 wR_2 = 0.0371	R_1 = 0.0418 wR_2 = 0.0636
Max. and min. transmission	0.558 and 0.458	0.634 and 0.353	0.881 and 0.449
[#] absolute structure (Flack) parameter: 0.025(5)			

or C carrier atoms by a factor of 1.2. The hydrogen atom for the solvent water molecule in the crystal structure of $[Pt(TU)_4]SiF_6 \cdot 0.25H_2O$ (with the oxygen being located in position *4a* of space group *P4/ncc*, no. 130) was taken from a difference fourier syntheses and not refined. The crystal used to determine the structure of **$[Pt(TU)_4](ClO_4)_2$** proved to be a pseudomerohedral twin. The application of an appropriate twin matrix (TWIN 1 0 0 0 –1 0 0 0 –1) resulted in a significant improvement of the refinement though the twinning was present only to a minor extent [BASF = 0.050(2)].

Crystallographic data and a summary of data collection and refinement parameters for all seven complexes are given in Table 9. For structure solution, refinement and graphical representations the SHELXTL NT 6.12 program package was used.[41]

CCDC-631060 (for **$[Pt(TU)_4]Cl_2$**), -631061 (for **$[Pt(TU)_4]I_2$**), -631062 (for **$[Pt(TU)_4](CF_3SO_3)_2$**), and -631063 (for **$[Pt(TU)_4](BPh_4)_2$**), -631064 (for **$[Pt(TU)_4](ClO_4)_2$**), -631065 (for **$[Pt(TU)_4]SiF_6 \cdot 0.25H_2O$**) and -631066 (for **$[Pt(TU)_4]S_2O_6$**) contain the supplementary crystallographic data for this paper. These data can be obtained free of charge from The Cambridge Crystallographic Data Centre via www.ccdc.cam.ac.uk/data_request/cif.

Supporting Information (see also the footnote on the first page of this article): Figures S1 to S3 present the molecular structure of the $[Pt(TU)_4]^{2+}$ cation in different complexes of the IIOO type.

Acknowledgments

The authors gratefully acknowledge financial support from the Deutsche Forschungsgemeinschaft (DFG) and thank Immo Weber, Dr. Nico van Eikema Hommes and Eike Hübner for fruitful discussions, and Christina Wronna for elemental analysis. ZDB thanks Deutscher Akademischer Austauschdienst (DAAD) for a fellowship. We also thank Prof. Tim Clark, Computer Chemistry Center and the Regionales Rechenzentrum Erlangen (RRZE) for computer time.

[1] A. F. Hollemann, N. Wiberg, *Lehrbuch der Anorganischen Chemie*, 101 ed., Walter de Gruyter, Berlin, New York, **1995**.
[2] B. Lippert (Ed.), *Cisplatin: Chemistry and Biochemistry of a Leading Anticancer Drug*, Wiley-VCH, Zurich, **1999**.
[3] P. M. Takahara, C. A. Frederick, S. J. Lippard, *J. Am. Chem. Soc.* **1996**, *118*, 12309–12321.
[4] N. Farrell, in *Transition Metal Complexes as Drugs and Chemotherapeutic Agents* (Eds.: R. Ugo, B. R. James), Kluwer, Dordrecht, The Netherlands, **1989**.
[5] Z. D. Bugarčić, G. Liehr, R. van Eldik, *J. Chem. Soc., Dalton Trans.* **2002**, 2825–2830.
[6] D. Jaganyi, A. Hofmann, R. van Eldik, *Angew. Chem. Int. Ed.* **2001**, *40*, 1680–1683.
[7] Z. D. Bugarčić, F. W. Heinemann, R. van Eldik, *Dalton Trans.* **2004**, 279–286.
[8] J. M. Berry, C. Jacobs, B. Sikic, J. Halsey, R. F. Borch, *J. Clin. Oncol.* **1990**, *8*, 1585–1590.
[9] M. Treskes, U. Holwerda, L. G. J. Nijtmans, H. M. Pinedo, W. J. F. Van der Vijgh, *Cancer Chemother. Pharmacol.* **1992**, *29*, 467–470.
[10] J. Filipski, K. W. Kohn, R. Prather, W. M. Bonner, *Science (Washington, DC, USA)* **1979**, *204*, 181–183.
[11] R. F. Ozols, B. J. Corden, J. Collins, R. C. Young, in *Platinum Coordination Complexes in Cancer Chemotherapy* (Eds.: M. P. Hacker, E. B. Douple, I. H. Krakoff), Martinus Nijhoff, Boston, **1984**, p. 321.
[12] J. H. Burchenal, K. Kalaher, K. Dew, L. Lokys, G. Gale, *Biochimie* **1978**, *60*, 961–965.
[13] J. Reedijk, *Chem. Rev.* **1999**, *99*, 2499–2510.
[14] R. L. Girling, K. K. Chatterjee, E. L. Amma, *Inorg. Chim. Acta* **1973**, *7*, 557–562.
[15] J. Arpalahti, B. Lippert, H. Schoellhorn, U. Thewalt, *Inorg. Chim. Acta* **1988**, *153*, 51–55.
[16] F. Boeckler, H. Lanig, P. Gmeiner, *J. Med. Chem.* **2005**, *48*, 694–709.
[17] T. C. Mak, Q. Li, *Adv. Mol. Struct. Res.* **1998**, *4*, 151–225.
[18] P. D. Beer, P. A. Gale, *Angew. Chem. Int. Ed.* **2001**, *40*, 486–516.
[19] C. R. Bondy, P. A. Gale, S. J. Loeb, *J. Supramol. Chem.* **2003**, *2*, 93–96.
[20] J. Calvo, J. S. Casas, E. Garcia-Martinez, Y. Parajo, A. Sanchez-Gonzalez, J. Sordo, *Z. Anorg. Allg. Chem.* **2004**, *630*, 215–216.
[21] V. Amendola, M. Boiocchi, L. Fabbrizzi, A. Palchetti, *Chem. Eur. J.* **2005**, *11*, 5648–5660.
[22] L. Fuks, N. Sadlej-Sosnowska, K. Samochoka, W. Starosta, *J. Mol. Struct.* **2005**, *740*, 229–235.
[23] P. A. Gale, M. E. Light, R. Quesada, *Chem. Commun.* **2005**, 5864–5866.
[24] P. A. Gale, M. E. Light, R. Quesada, *CrystEngComm* **2006**, *8*, 178–188.
[25] a) We tried to include solvent effects in our calculations by applying the IPCM and PCM solvent model as implemented in Gaussian 03. Due to well documented problems (see, for example ref.[25b,25c]), not all three species could be calculated. The obtained data suggest the same stability trends for the different conformers; b) P. Illner, A. Zahl, R. Puchta, N. J. R. van Eikema Hommes, P. Wasserscheid, R. van Eldik, *J. Organomet. Chem.* **2005**, *690*, 3567–3576; c) R. Puchta, T. Clark, W. Bauer, *J. Mol. Model.* **2006**, *12*, 739–747.
[26] G. R. Desiraju, *Angew. Chem.* **1995**, *107*, 2541–2558.
[27] For the consequences concerning possible enantimerization mechanisms see: R. Puchta, R. Meier, N. J. R. van Eikema Hommes, R. van Eldik, *Eur. J. Inorg. Chem.* **2006**, 4063–4067.
[28] A. D. Becke, *J. Chem. Phys.* **1993**, *98*, 5648–5652.
[29] C. Lee, W. Yang, R. G. Parr, *Phys. Rev. B: Condens. Matter* **1988**, *37*, 785–789.
[30] P. J. Stephens, F. J. Devlin, C. F. Chabalowski, M. J. Frisch, *J. Phys. Chem.* **1994**, *98*, 11623–11627.
[31] T. H. Dunning Jr, P. J. Hay, in *Modern Theoretical Chemistry* (Eds.: H. F. Schaefer III), Plenum, New York, **1976**, vol. 3, p. 1.
[32] W. R. Wadt, P. J. Hay, *J. Chem. Phys.* **1985**, *82*, 284–298.
[33] P. J. Hay, W. R. Wadt, *J. Chem. Phys.* **1985**, *82*, 270–283.
[34] P. J. Hay, W. R. Wadt, *J. Chem. Phys.* **1985**, *82*, 299–310.
[35] S. Huzinaga, *Gaussian Basis Sets for Molecular Calculations*, Elsevier, Amsterdam, **1984**.
[36] The performance of RB3LYP/LANL2DZp is well documented: a) S. Klaus, H. Neumann, H. Jiao, A. Jacobi von Wangelin, D. Goerdes, D. Struebing, S. Huebner, M. Hateley, C. Weckbecker, K. Huthmacher, T. Riermeier, M. Beller, *J. Organomet. Chem.* **2004**, *689*, 3685–3700; b) R. W. Saalfrank, C. Deutscher, H. Maid, A. M. Ako, S. Sperner, T. Nakajima, W. Bauer, F. Hampel, B. A. Hess, N. J. R. van Eikema Hommes, R. Puchta, F. W. Heinemann, *Chem. Eur. J.* **2004**, *10*, 1899–1905; c) A. Scheurer, H. Maid, F. Hampel, R. W. Saalfrank, L. Toupet, P. Mosset, R. Puchta, N. J. R. van Eikema Hommes, *Eur. J. Org. Chem.* **2005**, 2566–2574; d) M. Galle, R. Puchta, N. J. R. van Eikema Hommes, R. van Eldik, *Z. Phys. Chem.* **2006**, *220*, 511–523.
[37] a) The LACV3P basis set is a triple-zeta contraction of the LACVP basis set developed and tested at Schrödinger, Inc. LACV3P is based on the Hay–Wadt-ECPs [33–35] and on the 6-311G basis set; b) T. Clark, J. Chandrasekhar, G. W. Spitznagel, P. von Ragué Schleyer, *J. Comput. Chem.* **1983**, *4*, 294–301;

c) M. J. Frisch, J. A. Pople, J. S. Binkley, *J. Chem. Phys.* **1984**, *80*, 3265–3269; d) R. Krishnan, J. S. Binkley, R. Seeger, J. A. Pople, *J. Chem. Phys.* **1980**, *72*, 650–654; e) . A. D. McLean, G. S. Chandler, *J. Chem. Phys.* **1980**, *72*, 5639–5648; f) A. V. Mitin, J. Baker, P. Pulay, *J. Chem. Phys.* **2003**, *118*, 7775–7782.
[38] M. J. Frisch, G. W. Trucks, H. B. Schlegel, G. E. Scuseri, M. A. Robb, J. R. Cheeseman, J. A. Montgomery Jr, T. Vreven, K. N. Kudin, J. C. Burant, J. M. Millam, S. S. Iyengar, J. Tomasi, V. Barone, B. Mennucci, M. Cossi, G. Scalmani, N. Rega, G. A. Petersson, H. Nakatsuji, M. Hada, M. Ehara, K. Toyota, R. Fukuda, J. Hasegawa, M. Ishida, T. Nakajima, Y. Honda, O. Kitao, H. Nakai, M. Klene, X. Li, J. E. Knox, H. P. Hratchian, J. B. Cross, V. Bakken, C. Adamo, J. Jaramillo, R. Gomperts, R. E. Stratmann, O. Yazyev, A. J. Austin, R. Cammi, C. Pomelli, J. W. Ochterski, P. Y. Ayala, K. Morokuma, G. A. Voth, P. Salvador, J. J. Dannenberg, V. G. Zakrzewski, S. Dapprich, A. D. Daniels, M. C. Strain, O. Farkas, D. K. Malick, A. D. Rabuck, K. Raghavachari, J. B. Foresman, J. V. Ortiz, Q. Cui, A. G. Baboul, S. Clifford, J. Cioslowski, B. B. Stefanov, G. Liu, A. Liashenko, P. Piskorz, I. Komaromi, R. L. Martin, D. J. Fox, T. Keith, M. A. Al-Laham, C. Y. Peng, A. Nanayakkara, M. Challacombe, P. M. W. Gill, B. Johnson, W. Chen, M. W. Wong, C. Gonzalez, J. A. Pople, *Gaussian 03 Revision C.02*, Gaussian Inc., Wallingford CT, **2004**.
[39] A. Yamaguchi, R. B. Penland, S. Mizushima, J. T. Lane, C. Curran, J. V. Quagliano, *J. Am. Chem. Soc.* **1958**, *80*, 527–529.
[40] *SADABS 2.06*, Bruker AXS Inc., Madison WI, USA, **2002**.
[41] *SHELXTL NT 6.12*, Bruker AXS Inc., Madison WI, USA, **2002**.

Received: November 1, 2006
Published Online: February 22, 2007

